# Effects of compositional variations on the properties of superconducting $(Bi,Pb)_2Sr_2Ca_2Cu_3O_\delta$

S. M. Green, Yu Mei, A. E. Manzi, and H. L. Luo
*Department of Electrical and Computer Engineering, University of California, San Diego, La Jolla, California 92093*

R. Ramesh[a] and G. Thomas
*National Center for Electron Microscopy, Materials and Chemical Sciences Division, Lawrence Berkeley Laboratory, 1 Cyclotron Road, Berkeley, California 94720*

(Received 26 January 1989; accepted for publication 20 March 1989)

The results of a systematic study on compositional variations within the $Bi_{2-x}Pb_xSr_2Ca_2Cu_3O_\delta$ superconducting system are reported. It is found that a secondary phase (or phases), likely composed of Pb-Sr-Ca-Cu-O, forms when $x$ exceeds 0.35, indicating that this is an upper limit on the amount of Pb which replaces Bi. Varying the Sr:Ca or Bi:Ca ratio has dramatic effects on the resistive and magnetic properties. It is suggested that there is a very limited range of solution among the alkaline-earth elements. Bi occupying Ca sites is probably deleterious for both $T_c$ and the structural stability of the 2223 phase. Preliminary results on textured ceramic samples have yielded $J_c$ (77 K) as high as 580 A/cm$^2$.

## I. INTRODUCTION

At least three superconducting phases have been identified in the Bi-Sr-Ca-Cu-O system[1] satisfying the general polytypoid formula $Bi_2Sr_2Ca_{n-1}Cu_nO_\delta$ ($n = 1$, 2, and 3).[2–6] The three, referred to by their cation stoichiometry (e.g., 2201, 2212, and 2223, respectively), are termed polytypoids since the variation in composition is accommodated through structural changes.[7] As $n$ increases, the $c$ parameter of the tetragonal unit cell stretches ($\sim$24.6, $\sim$30.6, and $\sim$37.1 Å for $n = 1$, 2, and 3, respectively) to allow for the intercalation of additional $CaCuO_2$ layers while the $a$ and $b$ parameters remain essentially unchanged ($a \cong b \cong 5.4$ Å). Transmission electron microscope (TEM) images demonstrate that individual grains contain layers corresponding to a mixture of the polytypoids. Occasionally, layers which appear to be $n = 4$ are observed. The superconducting transition temperature ($T_c$) increases with $n$: $\sim$20, $\sim$80, and $\sim$110 K.[3–6] If $n > 3$ can be stabilized and prepared in quantities substantial enough for transport property measurements, the $T_c$ is predicted to increase.[8]

It is tempting to assert that the 2212 polytypoid is the most stable, forming readily over the temperature interval 850–870 °C. In a very narrow temperature range near the melting point ($\sim$880 °C), the 2223 phase begins forming as stacking faults within the 2212 matrix. By thoroughly grinding, carefully setting the sintering temperature, and controlling the cooling rate, quite a large fraction of the 2212 polytypoid can be converted to the 2223 form.[6,9,10] However, to our knowledge, single-phase $Bi_2Sr_2Ca_2Cu_3O_\delta$ bulk ceramics with zero resistance ($T_{c,0}$) substantially above 90 K have not been prepared. In samples prepared using standard solid-state sintering techniques, this phase does not appear to be energetically favored over the 2212 phase. The samples typically exhibit a resistive onset at $\sim$110 K with zero resistance generally attained at $\sim$75 K. In addition to a broadening of the resistive and magnetic transitions, as would be expected from proximity effects, clearly identifiable steps are observed indicating that regions of 2223 stoichiometry are separated from each other by a large distance compared with the superconducting coherence length. High-resolution TEM images have confirmed the propensity of the $n = 1$ and 2 polytypoids to form adjacent to grain boundaries, with layers corresponding to $n = 3$ found inside the grains.[11,12]

The 2223 polytypoid is stabilized by partially substituting Pb for Bi,[11,13] and $T_{c,0} > 105$ K can be attained easily in bulk ceramic samples.[14,15] The sintering temperature does not have to be as carefully controlled to produce material which is predominantly 2223, although preventing the formation of small amounts of the other polytypoids remains a challenge. Furthermore, TEM images indicate that 2223 grains free of the 2212 and 2201 stacking faults do form.[11] In a recent study, it is shown that Pb-substituted 2223 samples can be made virtually single-phase (i.e., step-free resistive and magnetic transitions along with powder x-ray diffraction patterns corresponding only to the 2223 phase), although the preparation requires considerable care.[16]

Within the Pb-free 2212 phase, there is a range of solid solution between Sr and Ca leading many researchers to describe its composition as $Bi_2(Sr,Ca)_3Cu_2O_\delta$.[2,17–19] This is reasonable since both are closely related alkaline-earth elements. Energy dispersive x-ray elemental microanalyses of individual grains indicate that some Ca can be replaced by Bi,[12] and the random occupation of Ca sites by Bi atoms in both the 2212 and 2223 polytypoids has been directly imaged.[20,21] That there should be a range of solution between Ca and Bi might seem strange at first glance; however, $Ca^{+2}$ and $Bi^{+3}$ have virtually identical ionic radii which makes the existence of such a solution rational. Such compositional variations seem to be a characteristic feature of this multicomponent oxide system.

In this systematic study, the range of nominal compositions within which the Pb-substituted 2223 phase is most stable was investigated. The maximum extent to which Pb replaces Bi is investigated employing x-ray diffraction, and

[a] Currently at Bell Communications Inc., 331 Newman Springs Rd., Red Bank, NJ 07701.

 0021-8979/89/140728-07$02.40  

peaks associated with a Pb-based impurity phase are identified. The effect of varying the Sr:Ca and Bi:Ca ratios on the resistive and magnetic properties of the sintered ceramics is also addressed. Electron microscopy is employed in an effort to correlate these effects with microstructural observations.

Lastly, we present preliminary results of transport critical current measurements at liquid-nitrogen temperature in zero applied field. A simple procedure is detailed for texturing bulk 2223 samples. The procedure is found to increase the critical current by a factor of 2–3 over unoriented samples.

## II. EXPERIMENTAL PROCEDURE

Three groups of compositional variants were explored. Samples within each group were prepared simultaneously, and are assumed to share identical thermal histories. The following nominal compositions were prepared:

Group A: $Bi_{2-x}Pb_xSr_2Ca_2Cu_3O_\delta$

$x = 0, 0.2, 0.4, 0.6, 0.8, 1, 1.5, 2;$

Group B: $Bi_{1.75}Pb_{0.25}Sr_{2-x}Ca_{2+x}Cu_3O_\delta$

$x = -0.50, -0.25, 0, 0.25, 0.50;$

Group C: $Bi_{1.75-x}Pb_{0.25}Sr_2Ca_{2+x}Cu_3O_\delta$

$x = -0.2, -0.1, 0, 0.1, 0.2.$

Appropriate weights of $Bi_2O_3$ (99.9%), PbO (99.999%), $SrCO_3$ (99.9%) or $SrO_2$ (99.5% dried overnight at 120 °C), $CaCO_3$ (99.95%) or CaO (99.95% dried at 200 °C), and CuO (99.95%) were ground together until no inhomogeneities were apparent. The purpose of Group A was to find out how much Pb could be introduced before Pb-based impurity phases began to form. For this group, $CaCO_3$ and $SrCO_3$ were chosen as alkaline-earth sources. $SrO_2$ and CaO were used in groups B and C. After calcining the powders overnight at 800 °C, the samples were thoroughly reground and pressed into 1-cm-diam pellets. Group A samples were sintered for 120 h at 845 °C with one intermediate regrinding, while groups B and C were sintered at 850 °C for 60 h with one intermediate regrinding. All samples were fired in air and were furnace cooled to room temperature.

Powder x-ray diffraction patterns were obtained using Ni-filtered Cu$K\alpha$ radiation ($\lambda = 1.5418$ Å) over the interval $20° \leqslant 2\theta \leqslant 50°$. Lattice parameters were computed using a least-squares fit to the most clearly identifiable peaks. Resistivity versus temperature curves ($\rho$ vs $T$) were measured on bars approximately $10 \times 2 \times 1$ mm$^3$ from room temperature down to 77 K in a simple $LN_2$ thermos. Contacts consisted of spring-loaded Rh-plated steel pogos pressed onto silver paint pads in the standard four-point configuration. About 1-mA rms current was supplied at 40 Hz with the sample's voltage drop detected by a lock-in amplifier. $T_{c,0}$ was defined as that temperature below which the lock-in could no longer detect the signal. The detection limit for typically sized samples was $\sim 0.5\ \mu\Omega$ cm. dc magnetic susceptibility data ($\chi$ vs $T$) was obtained using a superconducting quantum interference device (SQUID) magnetometer (Quantum Design MPMS) at 20 Oe over the temperature interval $10 \leqslant T \leqslant 150$ K on the same bars used for resistivity measurements. The temperature was lowered to 10 K in zero applied field, then the field was applied parallel to the sample's long axis. Data were collected as the sample was warmed to 150 K (shielding experiment) and cooled back down to 10 K (Meissner experiment). Since shape and density factors were not taken into account, these data are interpreted qualitatively. No attempt is made to estimate absolute volume fractions of superconducting phases, although volume ratios of the various superconducting phases in a given sample are addressed. Specimens for high-resolution TEM were prepared as described elsewhere.[5] The imaging was carried out in the Berkeley Atomic Resolution Microscope at 800 kV.

The specimens used for transport critical current measurements ($J_c$) had nominal composition $Bi_{1.5}Pb_{0.5}Sr_2Ca_2Cu_3O_\delta$ and were prepared using $Bi_2O_3$, PbO, $SrCO_3$, $CaCO_3$, and CuO. Several grams of the intimately mixed powders were calcined at 800 °C for 10 h, then reground and pressed into 2-cm-diam pellets. The pellets were sintered at 845 °C for 2 weeks with one intermediate regrinding, then furnace cooled to room temperature. Several bars were cut and sanded to 360 $\mu$m thickness for $\rho$ vs $T$ and $J_c$ characterizations.

The remainder was thoroughly reground, and textured as follows: Several 0.5-g portions were weighed and sprinkled into the 2-cm die such that a flat, even distribution of powder resulted. Uniaxial pressure was slowly increased to 5 kbar in order to allow the highly anisotropic platelets to flow and orient themselves. These thin (360 $\mu$m) disks were sintered at 825 °C for 48 h, then furnace cooled to room temperature. The preferred orientation was checked by obtaining the x-ray diffraction patterns from both surfaces. (However, the quality of orientation as a function of depth from the surface has not been determined.) Bars were cut from the disks for $\rho$ vs $T$ and $J_c$ measurements.

Low-resistance ohmic contacts for $J_c$ measurements were formed in the same fashion as described above with one additional step. The sample, with its freshly applied silver paint pads, was placed in a preheated furnace at 820 °C for 10 min. Then the furnace was turned off and allowed to cool to room temperature. The pogos were tightened into place, and the sample immersed in $LN_2$. The current, applied normal to the $c$ axis in textured samples, was ramped until 1 $\mu$V/cm was obtained. This value was used to compute $J_c$.

## III. RESULTS AND DISCUSSION

The powder x-ray diffraction pattern for the group A sample with $x = 0.6$ is displayed in Fig. 1. With the exception of the split peak centered near 31.3°, a peak near 44.7°, and several small peaks between 35° and 41°, this pattern can be indexed to a face-centered-tetragonal cell with dimensions $a \cong b \cong 5.40$ Å and $c \cong 37.10$ Å in excellent agreement with the reported lattice parameters of the 2223 phase devoid of Pb (Table I).[3,6]

In Fig. 2 we display the pattern for the group A sample with $x = 2.0$. This pattern matches the background pattern of the $x = 0.6$ pattern. Clearly, those peaks which do not index into the 2223 structure (Fig. 1) belong to a Pb-based impurity phase. The impurity peaks first appeared in the sample with $x = 0.4$. However, this sample also showed traces of the 2212 phase. This indicates that excess Pb con-

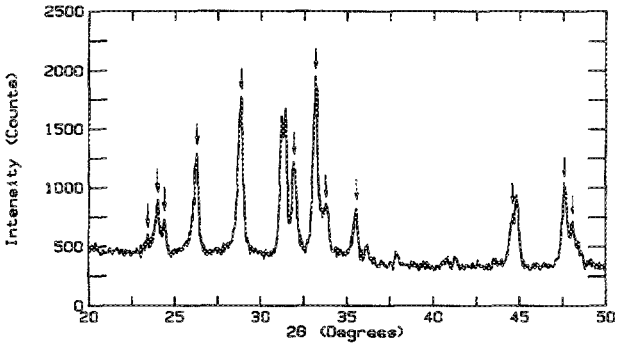


FIG. 1. Powder x-ray diffraction pattern for sample with nominal composition $Bi_{1.4}Pb_{0.6}Sr_2Ca_2Cu_3O_\delta$. The arrows indicate the peaks used to compute the lattice parameters and are summarized in Table I.

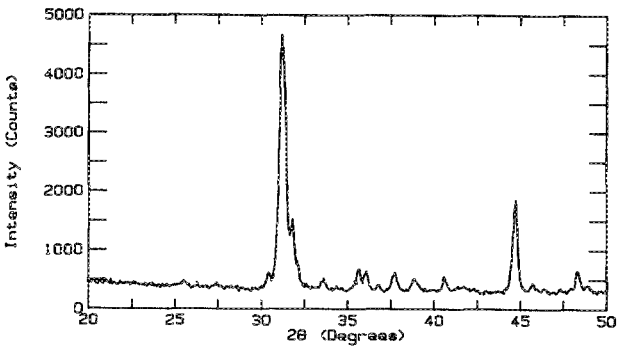


FIG. 2. Powder x-ray diffraction pattern for sample with nominal composition $Pb_2Sr_2Ca_2Cu_3O_\delta$.

tinues to discourage the formation of the 2212 phase without entering the 2223 structure. We estimate the saturation solubility of Pb in the 2223 phase as $x \approx 0.35$ in substantial agreement with microanalytical data. A typical energy-dispersive x-ray (EDX) spectrum from an $x = 0.6$ sample, along with the quantified composition, was presented in Ref. 12. The ratio Pb:Bi + Pb in that case was 0.18. Based on the nominal composition of the sample, the ratio should have been $x/2 = 0.3$. The fact that superconducting grains from samples nominally rich in Pb consistently show a maximum Pb:Bi + Pb ratio near 0.18 (corresponding to $x = 0.36$) and that an impurity phase first appears in the powder x-ray diffraction pattern at $x = 0.4$ is quite consistent. Grains composed of Pb-Sr-Ca-Cu-O have been identified in TEM images but have not been studied systematically.

The $\rho$ vs $T$ curves for group B samples are presented in Fig. 3 and the $\chi$ vs $T$ data are shown in Fig. 4. The sample most deficient in Ca ($x = -0.5$) barely displays a resistive kink above 100 K. The susceptibility data confirm that this kink is the result of a small fraction of the 2223 polytypoid. However, the x-ray pattern for this sample indicates the predominance of the 2212 polytypoid. Its normal-state resistivity [$\rho(T > T_c)$] is much lower than the other samples which is characteristic of the 2212 phase as compared to the 2223 phase. In Pb-free samples, the 2212 phase has $T_c \sim 80$ K while the majority of the diamagnetic transition for this sample is centered at $T \sim 65$ K with onset behavior beginning at $T \sim 68$ K. It has been demonstrated that the $T_c$ of the Pb-free 2212 phase can be varied from $\sim 70$ to $\sim 85$ K depending on the partial pressure of oxygen during sintering.[22] It is difficult to draw conclusions based on the available data; however, our results indicate that Pb suppresses the $T_c$ of the $n = 2$ polytypoid under the present preparation conditions.

Two of the samples ($x = -0.25$ and $x = 0$) attained zero resistance above 100 K without any apparent steps. For the sample with nominal 2223 stoichiometry, $T_{c,0} = 105$ K while for the sample slightly rich in Sr, $T_{c,0} = 108$ K. The susceptibility data give no clue as to the origin of this difference. Both samples demonstrate a sharp diamagnetic onset ($\chi < 0$) at $T_c = 111.5$ K, with an additional step evident in the shielding curves below 75 K. (A very slight step can be

TABLE I. Powder x-ray diffraction peaks used to calculate lattice parameters from Fig. 1.

| $h$ | $k$ | $l$ | $2\theta$ | $I_{obs}/I_0$ | $d_{obs}$ (Å) | $d_{calc}$ (Å) |
|---|---|---|---|---|---|---|
| 1 | 1 | 1 | 23.43 | 10 | 3.797 | 3.7985 |
| 0 | 0 | 10 | 23.98 | 29 | 3.711 | 3.7101 |
| 1 | 1 | 3 | 24.40 | 19 | 3.648 | 3.6486 |
| 1 | 1 | 5 | 26.25 | 57 | 3.395 | 3.3953 |
| 1 | 1 | 7 | 28.83 | 88 | 3.097 | 3.0982 |
| 0 | 0 | 12 | | | | 3.0918 |
| 1 | 1 | 9 | 31.94 | 53 | 2.802 | 2.8014 |
| 2 | 0 | 0 | 33.17 | 100 | 2.701 | 2.7001 |
| 0 | 0 | 14 | 33.77 | 28 | 2.654 | 2.6501 |
| 1 | 1 | 11 | 35.52 | 25 | 2.527 | 2.5279 |
| 2 | 0 | 12 | 44.60 | 23 | 2.032 | 2.0337 |
| 2 | 2 | 0 | 47.61 | 40 | 1.910 | 1.9093 |
| 1 | 1 | 17 | 48.06 | 19 | 1.893 | 1.8948 |
| 2 | 0 | 14 | | | | 1.8913 |

Lattice parameters fit: $a = 5.399(8)$ Å, $b = 5.400(7)$ Å, $c = 37.101(3)$ Å

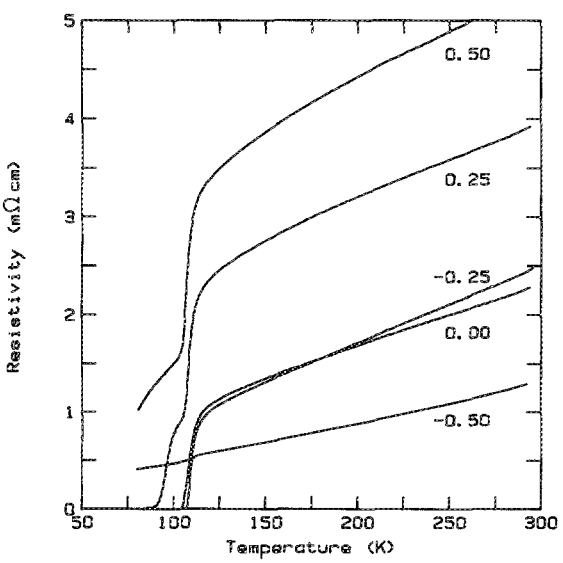


FIG. 3. $\rho$ vs $T$ curves for samples with nominal composition $Bi_{1.75}Pb_{0.25}Sr_{2-x}Ca_{2+x}Cu_3O_\delta$ ($x$ as indicated). Note the systematic increase in $\rho(T > T_c)$ with $x$ except between $x = -0.25$ and 0.

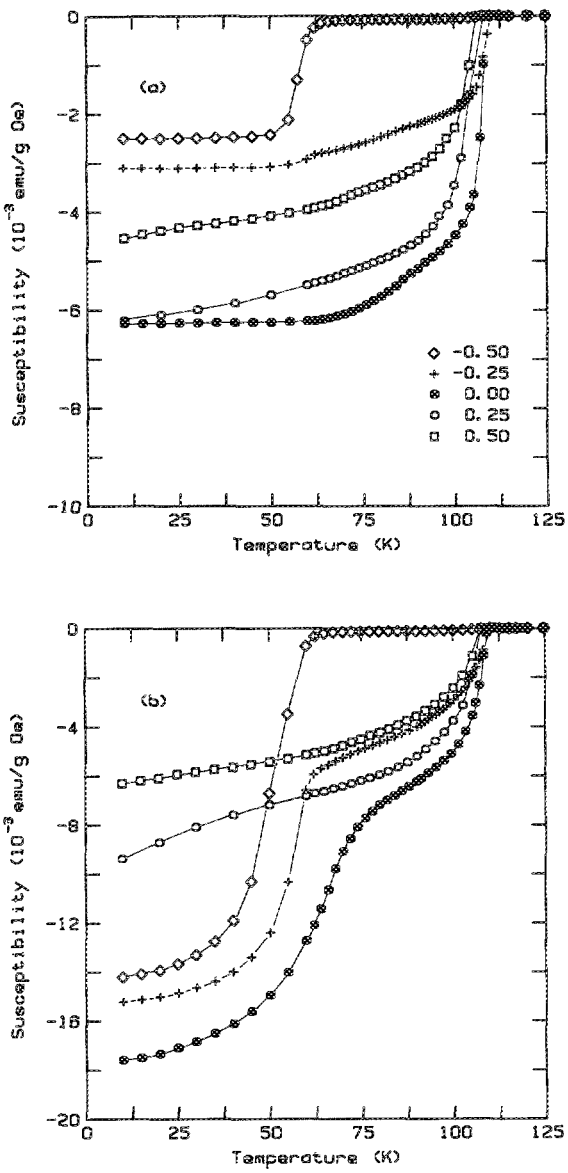


FIG. 4. (a) Meissner and (b) shielding data for samples with nominal composition $Bi_{1.75}Pb_{0.25}Sr_{2-x}Ca_{2+x}Cu_3O_\delta$ ($x$ as indicated).

delineated in the Meissner data of the $x = -0.25$ sample.) We associate this lower temperature step in the shielding data with the 2212 polytypoid which seems to form preferentially next to the grain boundaries in Pb-free samples. The fact that zero resistance was obtained well above 100 K indicates that a significant fraction of the superconducting grains are not separated from each other by a lower-$T_c$ polytypoid. Based on the meager to nonexistent step in the Meissner curves, the fraction is quite large.

The normal-state resistivity increases systematically with $x$ except between $x = -0.25$ and 0. Within this interval, the difference in the magnitude of the normal-state resistivity is within measurement error. $d\rho(T > T_c)/dT$ and $T_{c,0}$ are slightly larger for $x = -0.25$. One might interpret these observations as indicating a range of solid solution among Sr and Ca within the 2223 phase. In fact, slight Sr enrichment might be beneficial.

On the other hand, the samples deficient in Sr are severely affected with considerably larger values of $\rho$ in the normal state and stepped resistive transitions below $T_c$. The resistivity curves are reminiscent of Pb-free samples. The diamagnetic transitions are broader with the onsets reduced to $\sim 107$ K in both cases. It is clear that Ca enrichment at the expense of Sr is deleterious in terms of $T_c$ and the connectivity of the highest-$T_c$ material present. However, neither sample demonstrates a clear susceptive step over the interval $10 \leqslant T \leqslant 100$ K in either the Meissner or shielding data. This indicates that there is no detectable amount of material with a $T_c$ in the given range that could be responsible for the resistive step. The 2201 phase is rather difficult to prepare with $T_c > 10$ K, and often is semiconducting rather than metallic. Depending on the preparation conditions, it may or may not have a $T_c$.[6,23] Material which is nonsuperconducting and, perhaps, nonmetallic adjacent to the grain boundaries would explain the increasing normal-state $\rho$ with $x$ and $T_{c,0} \ll 100$ K even though a shoulder is not observed below 100 K in the diamagnetic response.

High-resolution TEM images of grain-boundary regions for samples with $x = -0.50$, $-0.25$, 0.25, and 0.50 are presented, respectively, in Figs. 5(a)–5(d). For the sample richest in Sr (a), the 2212 polytypoid is predominant up to the grain boundary, in full agreement with the results obtained using x-ray diffraction, $\rho$ vs $T$, and $\chi$ vs $T$ characterizations. The sample slightly rich in Sr (b) displays very little of the 2212 polytypoid with the 2223 phase contiguous up to the grain boundary, which is as expected given the step-free resistive transition with $T_{c,0} = 108$ K (Fig. 3). The image from the sample slightly rich in Ca (c) clearly demonstrates several layers of the 2201 polytypoid adjacent to the grain boundary. In this image, all four polytypoids are seen to coexist within the same grain. Between pairs of arrows, layers corresponding to the 2234 polytypoid can be found. While the occurrence of $n = 4$ is quite widespread in this image, our inability to delineate peaks in the powder x-ray diffraction pattern corresponding to the 2234 structure (with $c \approx 43.5$ Å) indicates that the fraction in the sample is very small. Thus, no conclusions can be drawn regarding the superconducting nature of these layers. In Fig. 5(d) we display an image from the sample richest in Ca. This particular grain demonstrates a random stacking of the $n = 2$ and $n = 3$ polytypoids with the two layers adjacent to the grain boundary identified as $n = 2$, followed by a single $n = 3$ layer, then several more $n = 2$ layers.

The $\rho$ vs $T$ and $\chi$ vs $T$ curves for group C samples are displayed in Figs. 6 and 7, respectively. All of these samples had room-temperature resistivities in the range 2.5–3.0 m$\Omega$ cm. For clarity, the $\rho$ data have been normalized to the room-temperature values. Both Bi-rich samples demonstrate stepped resistive transitions. The height of the step, $T_{c,0}$, and $d\rho/dT$ ($T > T_c$) all show systematic variation with decreasing $x$. The steps become quite clear and $T_{c,0}$ decreases monotonically as Bi + Pb:Ca exceeds 1. Upon examination of the Meissner data, the reason also seems quite clear: A shoulder at $T \sim 70$ K becomes progressively sharper with decreasing $x$. Thus, increasing the Bi concentration at the expense of Ca promotes the formation of the 2212 polyty-

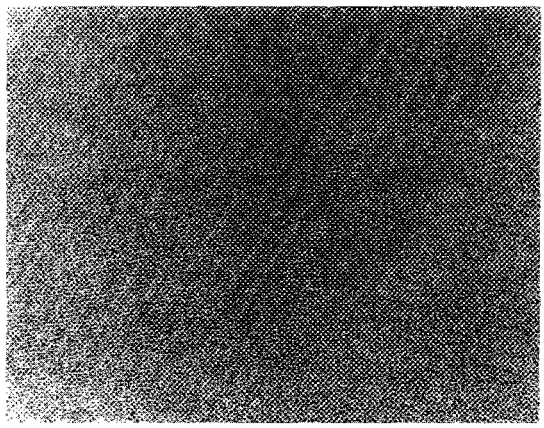

(a)

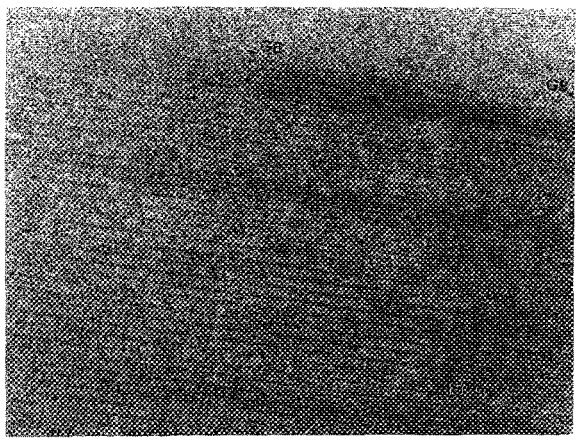

(c)

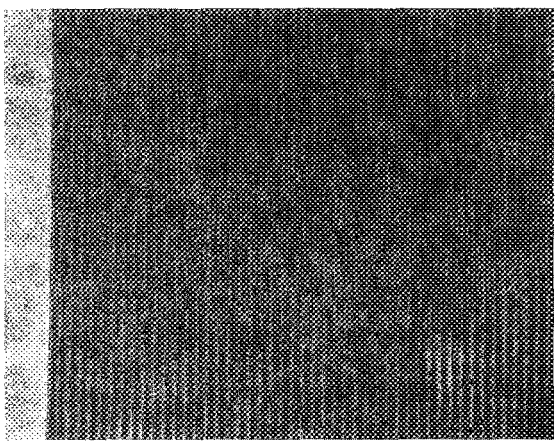

(b)

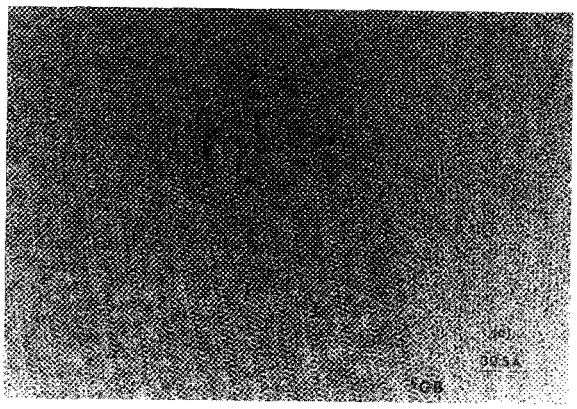

(d)

FIG. 5. High-resolution TEM images of regions adjacent to a grain boundary (GB) from samples with nominal composition $Bi_{1.75}Pb_{0.25}Sr_{2-x}Ca_{2+x}Cu_3O_\delta$. (a) For $x = -0.5$, essentially 2212 is observed. (b) For $x = -0.25$, the 2223 phase forms up to the grain boundary with no apparent stacking faults. (c) For $x = 0.25$, all four polytypoids coexist within the same grain. Next to the grain boundary at least five layers of 2201 can be found. Layers corresponding to $n = 4$ are located between pairs of arrows. (d) In this image from the $x = 0.5$ sample, a single layer of 2223 interrupts the 2212 sequence near the grain boundary.

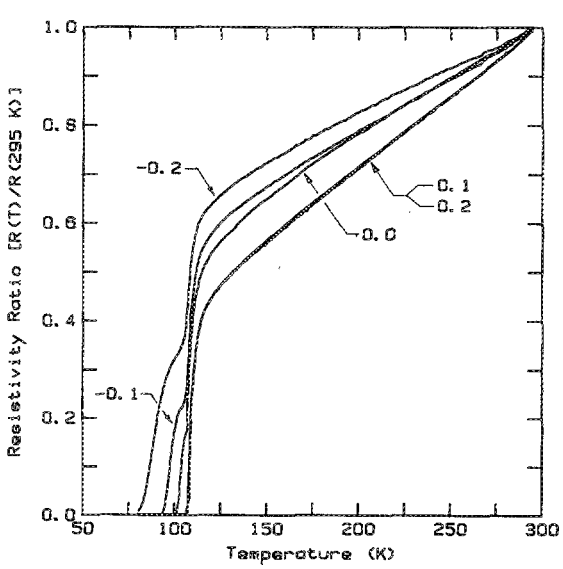


FIG. 6. $\rho$ vs $T$ curves for samples with nominal composition $Bi_{1.75-x}Pb_{0.25}Sr_2Ca_{2+x}Cu_3O_\delta$ ($x$ as indicated).

poid. The interpretation is reasonable since the 2212 polytypoid is rich in Bi and deficient in Ca as compared to the 2223 polytypoid. Bi occupying Ca sites may induce the 2223 structure to collapse into the 2212 structure with a concommitant suppression of $T_{c,0}$. Such a situation would most likely occur adjacent to grain boundaries.

The resistivity curves of the two samples with Bi + Pb:Ca less than 1 both demonstrate step-free transitions with $T_{c,0} = 107$ K. The situation is considerably different from that of group B samples with Sr:Ca less than 1. In both cases, the samples are Ca rich. Yet, if the Ca enrichment is at the expense of Sr, intergranular connectivity is frustrated, while if it is at the expense of Bi, then the 2223 material is contiguous. In particular, the shielding curves show a stepped diamagnetic response in the former which becomes more pronounced with increasing $x$, but a step-free response in the latter. This serves to emphasize that the nature of the resistive transition does not correlate well with the magnetic transition in this complicated oxide system. A step in the diamagnetic response does not imply a stepped resistive transition, and a step-free susceptibility curve does not guar-

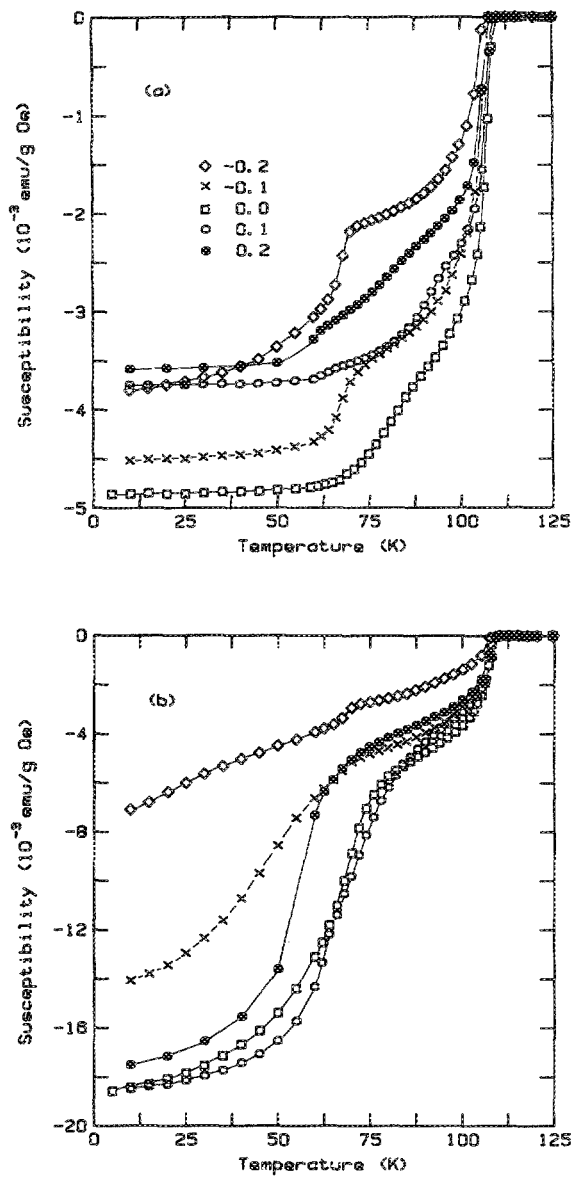


FIG. 7. (a) Meissner and (b) shielding data for samples with nominal composition $Bi_{1.75-x}Pb_{0.25}Sr_2Ca_{2+x}Cu_3O_\delta$ ($x$ as indicated).

antee a step-free resistive transition. The magnetic data provide information regarding the relative amounts of the various superconducting phases present. The resistivity curves indicate how well the highest-$T_c$ regions connect to each other. The idea of grain-boundary layers composed of a lower $T_c$, normal metallic, or semiconducting polytypoid is consistent with intergranular weak link interpretations. When the boundary layers are thick enough, clear steps in the $\rho$ vs $T$ curves emerge. Since the coherence length parallel to the $c$ axis is thought to be of the order 10 Å, even a couple of "weakened" layers could have substantial effect on the resistivity and shielding data with minimal consequences for the Meissner data.

The Meissner data for groups B and C indicate that the nominal 2223 composition, with equal atomic ratios of Bi + Pb, Sr, and Ca, is close to optimum. In Fig. 4(a), the $x = 0$ curve has the highest onset temperature with the least broadening below 100 K. Similarly, the $x = 0$ curve in Fig. 7(a) is superior in terms of onset temperature, broadening, and shoulders. The 2223 Meissner signals for samples from both groups, however, show significant tails to well below 75 K, perhaps indicating a range of $T_c$'s dependent on an unidentified, processing-dependent parameter. For example, it has been demonstrated that the $T_c$ of the Pb-free 2212 phase is sensitive to the partial pressure of oxygen in the furnace and is maximized near 10-mbar $O_2$, significantly below atmospheric concentrations.[22] If the parameter is the amount of intercalated oxygen, we would expect the grain-boundary region to behave differently than the interior of the grains due to oxygen diffusion via grain boundaries. Small steps, such as those observed in the $\rho$ vs $T$ curve for the $x = 0$ sample from group C, could be a manifestation of this possibility, and would depend sensitively on the cooling rate.

Lastly, the x-ray diffraction pattern off the surface of a textured $Bi_{1.5}Pb_{0.5}Sr_2Ca_2Cu_3O_\delta$ disk is displayed in Fig. 8. The hundred-fold increase in the intensity of the $00l$ peaks as compared to the powder pattern (Fig. 1) attests to the degree of alignment achieved through this simple preparation procedure. The $\rho$ vs $T$ curves for an unoriented and a textured specimen are shown in Fig. 9. The unoriented sample had $J_c$ (77 K) = 280 A/cm$^2$ and the textured sample had $J_c$ (77 K) = 580 A/cm$^2$. While these are the highest values obtained from this batch, it should be noted that none of our textured samples have had $J_c$ (77 K) below 400 A/cm$^2$ and most of our untextured samples have had $J_c$ (77 K) $\approx$200 A/cm$^2$. Considering the large structural anisotropy, such an improvement is not unexpected. Ceramic $YBa_2Cu_3O_7$ samples prepared by similar solid-state methods typically have $J_c$ (77 K) significantly less than these values. The increased $T_c$ in concert with greater structural anisotropy may allow superior properties to be realized in Bi-Pb-Sr-Ca-Cu-O ceramics.

## IV. CONCLUSION

In this study, we have demonstrated that the range of $x$ in $Bi_{2-x}Pb_xSr_2Ca_2Cu_3O_\delta$ is limited to approximately $0 \leqslant x \leqslant 0.35$. Roughly 1 in 6 Bi sites can be occupied by Pb. When this value is exceeded, an impurity which is most like-

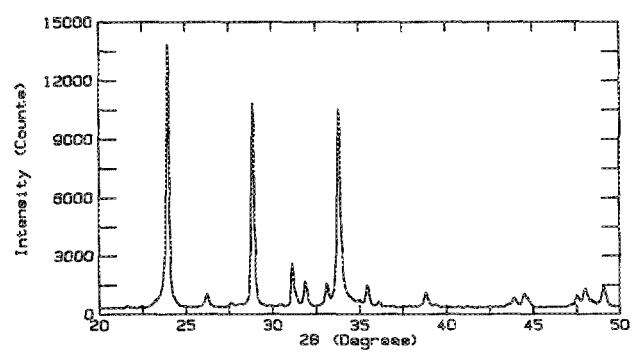


FIG. 8. X-ray diffraction pattern taken from the surface of a textured $Bi_{1.5}Pb_{0.5}Sr_2Ca_2Cu_3O_\delta$ ceramic disk.

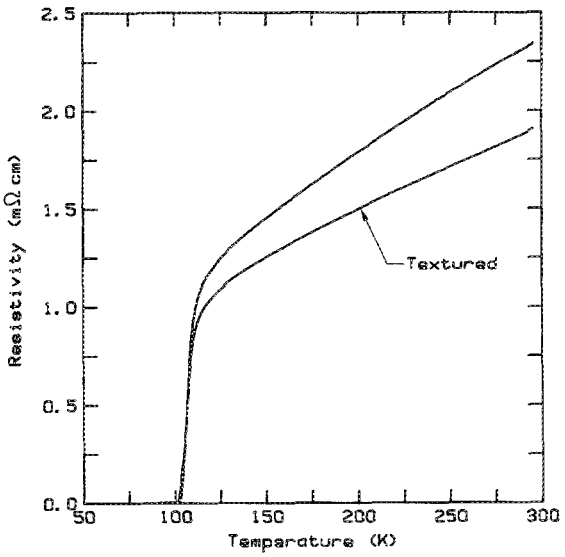


FIG. 9. $\rho$ vs $T$ curves for an unoriented and a textured sample with nominal composition $Bi_{1.5}Pb_{0.5}Sr_2Ca_2Cu_3O_\delta$.

ly composed of Pb-Sr-Ca-Cu-O readily forms. The appropriate sintering temperature decreases from ~880 to 845 °C as $x$ increases from 0 to 0.35.

The nominal 2223 stoichiometry yields the sharpest diamagnetic transitions indicating that the optimized stoichiometry has Sr:Ca and Bi + Pb:Ca very close to 1. A range of solid solution probably exists among Sr and Ca with Sr likely occupying Ca sites. In this case, we can generalize the composition to $Bi_{2-x}Pb_xSr_2Ca_{2-y}Sr_yCu_3O_\delta$ with $0 \leqslant x \leqslant 0.35$ and $0 \leqslant y \leqslant 0.25$ as the approximate ranges. Slight Sr enrichment may sharpen the transition to the superconducting state. When the ratios Bi + Pb:Sr:Ca stray too far from 1:1:1, stepped resistive transitions result. The appearance of the steps correlates well to the observation of grain-boundary layers with $n = 1$ or 2.

The large structural anisotropy allows for significant alignment of the grains in the sintered ceramic. The $c$ axes align parallel to the direction of an applied uniaxial force if the force is slowly increased so as to allow the grains to flow and orient. As a consequence, the transport $J_c$ perpendicular to the $c$ direction is found to increase by a factor of 2–3 over that obtained for unoriented samples.

## ACKNOWLEDGMENTS

The work at U. C. San Diego is supported by the California MICRO program and Hughes Aircraft Company. The work at Lawrence Berkeley Laboratory is supported by the Director, Office of Energy Research, Office of Basic Energy Sciences, Materials Sciences Division of the U.S. Department of Energy under Contract No. DE-AC03-76SF00098.

[1]M. Maeda, Y. Tanaka, M. Fukutomi, and T. Asano, Jpn. J. Appl. Phys. Lett. **27**, L209 (1988).
[2]M. A. Subramanian, C. C. Torardi, J. C. Calabrese, J. Gopalakrishnan, K. J. Morrissey, T. R. Askew, R. B. Flippen, U. Chowdhry, and A. W. Sleight, Science **239**, 1015 (1988).
[3]H. W. Zandbergen, Y. K. Huang, M. J. V. Menken, J. N. Li, K. Kadowaki, A. A. Menovsky, G. van Tendeloo, and S. Amelinckx, Nature **332**, 620 (1988).
[4]R. Ramesh, G. Thomas, S. M. Green, M. L. Rudee, and H. L. Luo, Appl. Phys. Lett. **53**, 520 (1988).
[5]R. Ramesh, C. J. D. Hetherington, G. Thomas, S. M. Green, C. Jiang, M. L. Rudee, and H. L. Luo, Appl. Phys. Lett. **53**, 615 (1988).
[6]J. M. Tarascon, W. R. McKinnon, P. Barboux, D. M. Hwang, B. G. Bagley, L. H. Greene, G. Hull, Y. LePage, N. Stoffel, and M. Giroud, Phys. Rev. B **8**, 8885 (1988).
[7]G. van Tendeloo, K. T. Faber, and G. Thomas, J. Mater. Sci. **18**, 525 (1988).
[8]F. Herman, R. V. Kasowski, and W. Y. Hsu, Phys. Rev. B **38**, 204 (1988).
[9]S. M. Green, Yu Mei, C. Jiang, H. L. Luo, and C. Politis, Mod. Phys. Lett. B **2**, 915 (1988).
[10]Yu Mei, S. M. Green, C. Jiang, and H. L. Luo, J. Appl. Phys. **64**, 6795 (1988).
[11]R. Ramesh, G. Thomas, S. M. Green, C. Jiang, Y. Mei, M. L. Rudee, and H. L. Luo, Phys. Rev. B **38**, 7070 (1988).
[12]R. Ramesh, G. Thomas, S. M. Green, Y. Mei, C. Jiang, and H. L. Luo, Appl. Phys. Lett. **53**, 1759 (1988).
[13]R. J. Cava, B. Batlogg, S. A. Sunshine, T. Siegrist, R. M. Fleming, K. Rabe, L. F. Schneemeyer, D. W. Murphy, R. B. van Dover, P. K. Gallagher, S. H. Glarum, S. Nakahara, R. C. Farrow, J. J. Krajewski, S. M. Zahurak, J. V. Waszczak, J. H. Marshall, P. Marsh, L. W. Rupp, Jr., W. F. Peck, and E. A. Rietman, Physica C **153-155**, 560 (1988).
[14]S. M. Green, C. Jiang, Y. Mei, H. L. Luo, and C. Politis, Phys. Rev. B **38**, 5016 (1988).
[15]B. W. Statt, Z. Wang, M. J. G. Lee, J. V. Yakhmi, P. C. de Camargo, J. F. Major, and J. W. Rutter, Physica C **156**, 251 (1988).
[16]Y. Mei, S. M. Green, C. Jiang, and H. L. Luo (in press).
[17]J. M. Tarascon, Y. LePage, P. Barboux, B. G. Bagley, L. H. Greene, W. R. McKinnon, G. W. Hull, M. Giroud, and D. M. Hwang, Phys. Rev. B **37**, 9382 (1988).
[18]Z. Iqbal, H. Eckhardt, F. Reidinger, A. Bose, J. C. Barry, and B. L. Ramakrishna, Phys. Rev. B **38**, 859 (1988).
[19]G. S. Grader, E. M. Gyorgy, P. K. Gallagher, H. M. O'Bryan, D. W. Johnson, Jr., S. Sunshine, S. M. Zahurak, S. Jin, and R. C. Sherwood, Phys. Rev. B **38**, 757 (1988),
[20]C. J. D. Hetherington, R. Ramesh, M. A. O'Keefe, R. Kilaas, G. Thomas, S. M. Green, and H. L. Luo, Appl. Phys. Lett. **53**, 1016 (1988).
[21]R. Ramesh, G. Thomas, S. M. Green, Y. Mei, M. L. Rudee, and H. L. Luo (unpublished).
[22]D. E. Morris, C. T. Hultgren, A. G. Markelz, J. Y. T. Wei, N. G. Asmar, and J. H. Nickel, Phys. Rev. B **39**, 6612 (1989).
[23]C. Michel, M. Hervieu, M. M. Borel, A. Grandin, F. Deslandes, J. Provost, and B. Raveau, Z. Phys. B **68**, 421 (1987).